IMPACT: International Journal of Research in Applied, Natural and Social Sciences (IMPACT: IJRANSS)
ISSN(P): 2347-4580; ISSN(E): 2321-8851
Vol. 4, Issue 10, Oct 2016, 5-16

SYNTHESIS, STRUCTURAL AND OPTICAL PROPERTIES OF NI-DOPED ZnO NANORODS PREPARED BY THE CO-PRECIPITATION METHOD

A.A.GADALLA[1], I.ABOOD[2] & M.M.ELOKR[3]

[1, 2] Department of Physics, Faculty of Science, Assuit University, Assuit, Egypt

[3]Department of Physics, Faculty of Science, Al-Azhar University, Cairo, Egypt

ABSTRACT

Zinc oxide nanorods and diluted magnetic semiconducting Ni-doped ZnO nanorods had been prepared byco-precipitation method. This method is straightforward and costs powerful. Ni-doped and undoped ZnO of trendy components nanoparticles $Zn_{1-x}Ni_xO$, (where x = 0, 0.02, 0.04, 0.05, 0.06 and 0.08) were correctly synthesized by co-precipitation approach. The structure and the optical properties of obtained samples have been investigated using X-ray Diffraction (XRD), energy dispersive X-ray spectroscopic analysis (EDX), Transmission Electron Microscope (TEM) and UV–visible absorption spectroscopy.

XRD patterns of doped samples display that the lattice constants of $Zn_{1-x}Ni_xO$, of $x > 0.0$ are slightly larger than the ones of pure ZnO. However, XRD reveals that both exhibit hexagonal wurtzite structure. The energy band gap has also been estimated using measured UV-VIS optical absorption spectra. EDX spectroscopy was used to identify the elemental constituents of a material. Also, TEM investigations give further insight to the morphology and the structural features of Ni-doped ZnO nanorods.

KEYWORDS: Nanocrystals, Co-Precipitation Method, Optical Properties, XRD, EDX, TEM

INTRODUCTION

In a previous couple of decades, metal oxide nanoparticles had been significantly investigated because of their atypical applications in the subject of spintronics [1], photo electronic [2], sensor [3], lasing devices [4] and light emitting diodes [5], etc. Zinc oxide (ZnO) is a transparent n-type semiconductor with a band gapof3.37eV.ZnO nano-particles acquired superb attention because of their unique catalytic, electrical, gas sensing, and optical properties [6-9]. Nickel oxide (NiO) is a transparent p-type semiconductor with a wide bandgap in the range of 3.6–3.8 eV [6, 10, 11]. Wide band-gap oxide semiconductors, when doped with transition metal ions (Mn, Fe, Co, and Ni) have attracted great deal interest for their promising versatile applications [12].Diluted Magnetic Semiconductors (DMS) shape a brand new class of magnetic substances, which fill the gap between ferromagnets and semiconductors [13].Doping of ZnO with magnetic ions induces magnetic properties, allowing awide range of applications [14]. Currently, a few effects have been performed regarding the room-temperature (RT) ferromagnetism, as predicted theoretically, in Ni-doped ZnO [15, 16]. Furthermore, Ni^{2+} (0.69Åhas the equal valence in comparison to Zn^{2+} and its radius is close to Zn^{2+} (0.74Å), so it is possible for Ni^{2+} sub-lattice to replace Zn^{2+} in ZnO lattice. some researches on Ni-doped ZnO had been stated and several effects showed that the one of a kind houses of ZnO has been changed after putting Ni into ZnO matrix [17, 18].

Various chemical techniques were evolved to prepare nanoparticles of different materials of interest. Most of the ZnO crystals had been synthesized by a conventional high-temperaturesolid-state method, wherein, it's miles hard to govern the particle properties and additionally, energy ingesting. ZnO nanoparticles can be prepared on a huge scale at low cost by simple solution based method, such as chemical precipitation, sol-gel synthesis, and hydrothermal reaction [19-24]. Co-precipitation is the name given by analytical chemists to a phenomenon whereby the fractional precipitation of a specified ion in a solution results in the precipitation not only of the target ion but also of other ions existing side by side in the solution [25].

Within the present paper, we will report the synthesis of Ni-doped ZnO in the form of nanoparticles that are investigated the use of X-ray diffraction (XRD), energy dispersive x-ray spectroscopy (EDX) and UV-Visible spectrometer.

EXPERIMENTAL

Samples Preparation

The DMS Samples of ($Zn_{1-x}Ni_xO$) have been prepared the use of the chemical precipitation method. The beginning materials Zn (Ch_3Coo) $_2H_2O$ and Ni (Ch_3Coo) $_4H_2O$had been blended then PVP introduced with a value. The stoichiometric quantity of Zinc acetate ($Zn(Ch_3Coo)2H_2O$) and Nickel acetate ($Ni(Ch_3Coo)4H_2O$) are dissolved in distilled water with (1gm) of *poly*-vinylpyrrolidone(PVP) and kept in a magnetic stirrer for five hours. The experiment was performed at room temperature. The final ingots have been dried at 70 ˚C for one day and annealed at 300 ˚C for six hours.

RESULTS AND DISCUSSIONS

Structural Determination

X-ray diffraction (XRD) patterns of $Zn_{1-x}Ni_xO$ (x=0, 0.02, 0.04, 0.05, 0.06, 0.08) are shown in Figure 1. The located peaks imply that all samples are having polycrystalline nature with hexagonal wurtzite shape. The found peaks are corresponding to (100), (002), (101), (102), (110) and (103) planes. The d-spacing of the peaks are properly matched with widespread records (JCPDS: 01-079-0208) for (x=0.00) and (JCPDS: 01-075-2820) for (x=0.02, 0.04, 0.05, 0.06, 0.08). No impurity phase turned into finding within the Ni-doped ZnO sample due to the smaller ionic radii of the Ni^{2+} ions (ionic radius: 0.69 Å) are easily substituted within the internal of Zn^{2+} ions (ionic radius 0.74 Å) [26,27]. The XRD patterns of Ni-doped ZnO are similar to that of pure ZnO.

It’s far obtrusive from XRD spectra that there is no existence for the peaks corresponding to Ni, oxides of Ni, Zn or Ni related secondary and impurity phases. Despite the fact that, there aren't any secondary phases detected with the aid of XRD analysis, the existence of secondary phases cannot be completely excluded due to the limitation of this characterization approach [28]. We are able to conclude that the doping of Ni does not change the wurtzite structure of ZnO and hence Ni^{2+} substitutes Zn^{2+} site into the crystal lattice.

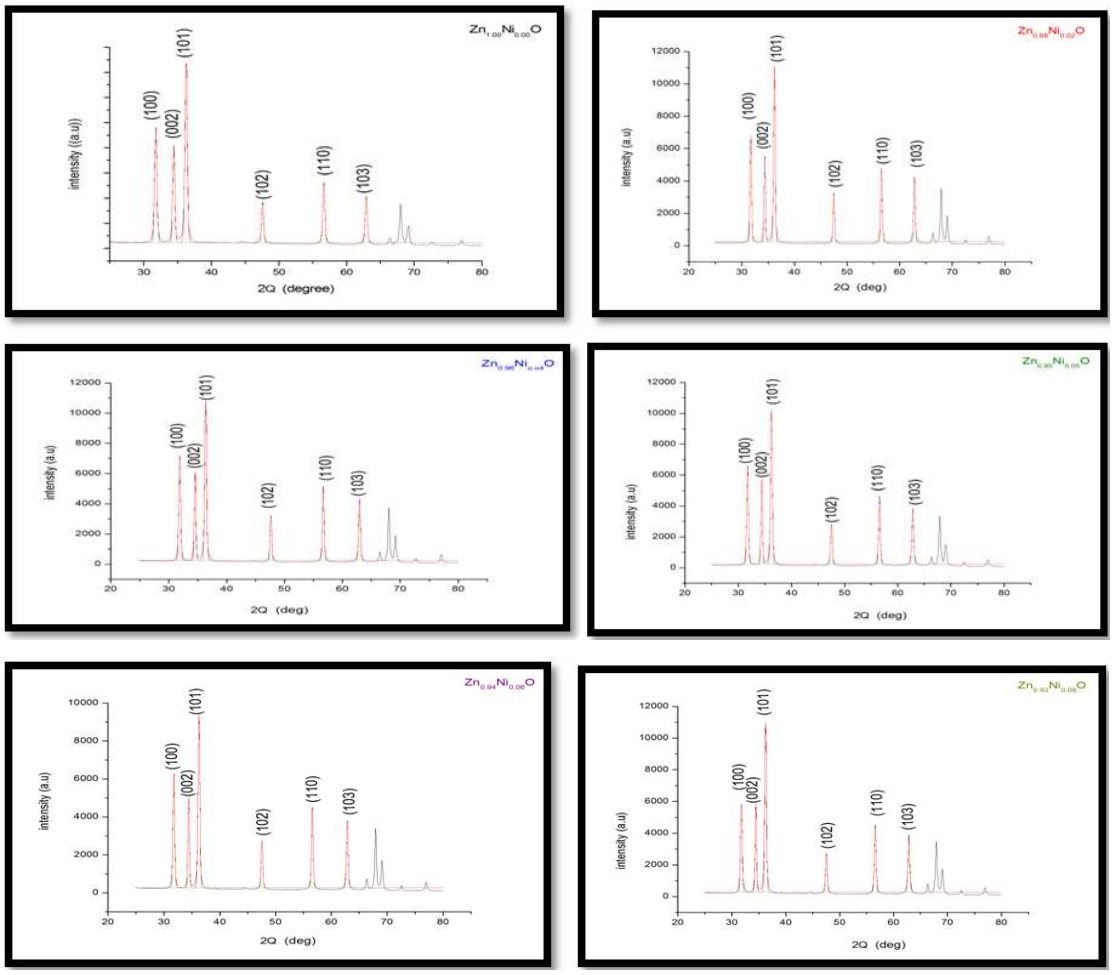

Figure 1: XRD Pattern of $Zn_{1-x}Ni_xO$, (where x = 0, 0.02, 0.04, 0.05, 0.06 and 0.08) at 300^{O}C

The average crystal size of the samples is calculated after appropriate background correction from X-ray line broadening of the diffraction peaks of (101) plane using Debye–Scherrer's formula [29].

$$Average\ crystal\ size\ (D_{hkl}) = \frac{0.9\,\lambda}{(\beta_{hkl}\times\cos\theta)} \quad \textbf{(1)}$$

Where, λ is the wavelength of X-ray used (1.5408 $A°$), β is the angular peak width at half maximum in radian along (101) plane, and θ is the Bragg's diffraction angle.

ZnO has hexagonal structure, the plane spacing is related to the lattice constants (a, c) and the Miller indices by the following relation:

$$\frac{1}{d_{hkl}^2} = \frac{4}{3}\left(h^2 + hk + \frac{k^2}{a^2}\right) + \frac{l^2}{c^2} \quad \textbf{(2)}$$

The micro-strain (ε) can be calculated using the formula [30],

$$\varepsilon = \frac{(\beta_{hkl}\times\cos\theta)}{4} \quad \textbf{(3)}$$

Table1. Cell Parameters 'a' and 'c', 'c/a' Ratio, Average Crystal Size (D) and Micro-Strain (ε) of Different $Zn_{1-x}Ni_xO$ Samples

% of Doping of Ni	$C_{(002)}$nm	$a_{(101)}$nm	c/a	D	$\varepsilon(10^{-3})$
0.00	0.52042333	0.32499537	1.601325	27.16298	1.151152
0.02	0.52170843	0.32579177	1.601355	29.72556	1.04677
0.04	0.5192144	0.3241018	1.60201	29.80187	1.046829
0.05	0.52119327	0.32548132	1.6013	27.79042	1.11996
0.06	0.52064163	0.32506656	1.601646	29.01175	1.074859
0.08	0.52076882	0.3252187	1.601288	28.02397	1.298611

The observed data reveal that lattice parameters 'a' and 'c' are almost composition independent. This can easily be accounted for the small difference between the ionicradius of Zn and Ni.

The Energy Dispersive X-ray Spectroscopic Analysis (EDX)

The EDX spectroscopy is used to analyze the chemical composition of grain sample. Also is used to product maps of elements, place, concentration, and distribution.

To confirm the presence of Ni ions in the synthesized nanoparticle ZnO,EDX measurements were done for all samples $Zn_{1-x}Ni_xO$ for (x=0.00, 0.02, 0.04, 0.05, 0.06, 0.08) figure 2. It is determined that there is two peaks belong to Zn and Ni, through growing Ni concentration in samples heights of its peak increase.

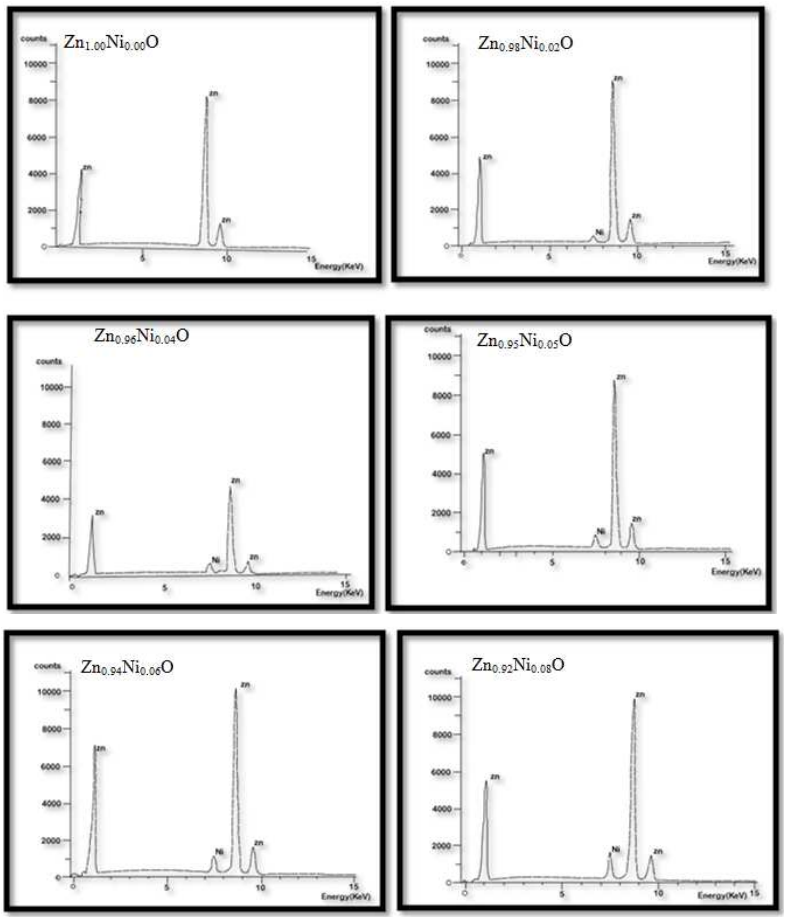

Figure 2: EDX Pattern of $Zn_{1-x}Ni_xO$, (where x = 0, 0.02, 0.04, 0.05, 0.06 and 0.08)

The data of EDX spectroscopy are presented in table 2. EDX spectra show good agreement with the experimental concentration used for $Zn_{1-x}Ni_xO$ samples.

Table 2: The Percentage of Ni in Different $Zn_{1-x}Ni_xO$ Samples Using EDX Analysis

Samples	Percentage of the Elements % Atomic(%)		
	Zn	Ni	Ni/Zn Ratio
ZnO	100.0	-	-
$Zn_{0.98}Ni_{0.02}O$	98.13	1.87	0.019
$Zn_{0.96}Ni_{0.04}O$	96.32	3.86	0.038
$Zn_{0.95}Ni_{0.05}O$	59.40	4.60	0.048
$Zn_{0.94}Ni_{0.06}O$	49.55	5.5	0.058
$Zn_{0.92}Ni_{0.08}O$	93.4	6.89	0.073

Transmission Electron Microscope (TEM)

As proven in Figure. 3, the TEM image of Ni (0.08, 0.05, 0.02) doped ZnO symbolizes nanorods. in step with the TEM image in Figure. 3(b), the diameter of the nanorod is ~ 48 nm. The "d" value indicating (002) plane of the hexagonal structure of ZnO is obtained as 0.264 nm. The HR-TEM image of undoped ZnO has already been reported and the "d" value is 0.260 nm [31]. The slight increase in the "d" value of Ni-doped ZnO is due to the smaller ionic radius of Ni^{2+} than that of Zn^{2+}. This change in lattice parameter was also observed and reported in Ni-doped ZnO [32].

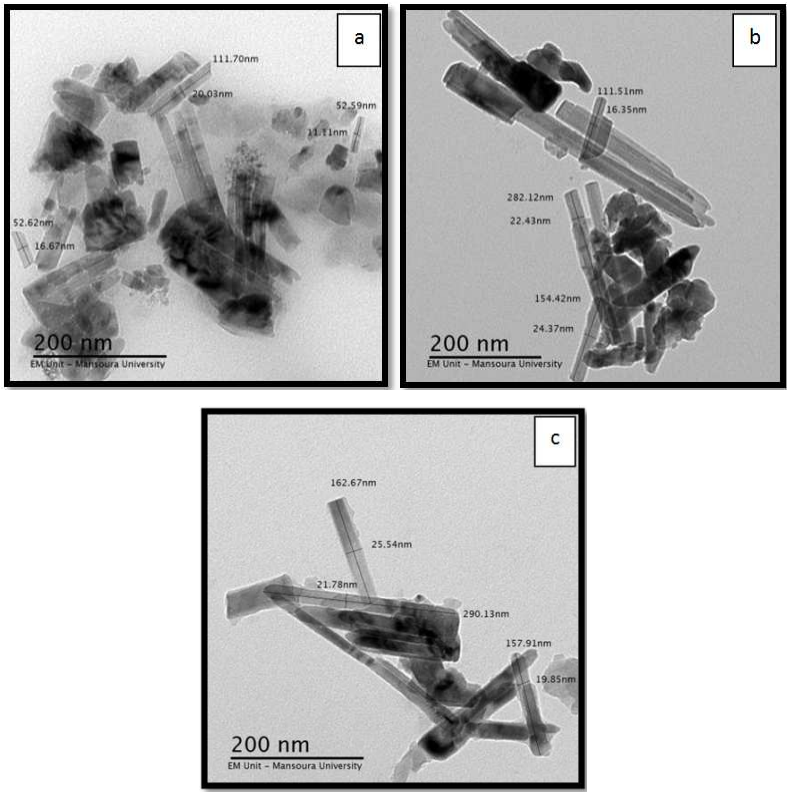

Figure 3: TEM Images of $Zn_{1-x}Ni_xO$, (where x = 0.02, 0.05and 0.08)

OPTICAL PROPERTIES

UV-Visible spectroscopy

The optical absorption spectra of undoped and Ni-doped ZnO (where x = 0.00, 0.02, 0.04, 0.05, 0.06, 0.08) samples in the variety of 300 to 800 nm were measured. The measurement was carried out using (LAMBDA 35) UV-Vis spectrophotometer. Optical absorption spectra of the measured samples are shown in Figure 4.

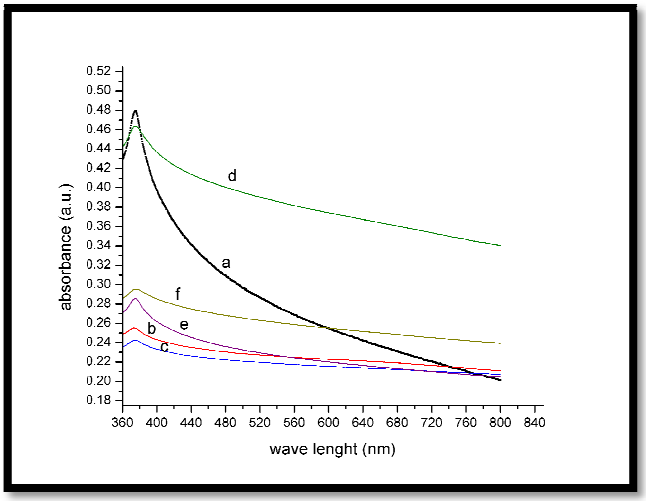

Figure 4: Absorbance Spectra of $Zn_{1-x}Ni_xO$, Samples: (a) x=0.00; (b) x=0.02; (c) x=0.04; (d) x=0.05; (e) x=0.06 and (f) x=0.08 as a Function of Wavelength

All samples observe not unusual pattern, wherein a single sharp absorption peak is found inside the UV region. Moreover, the placement of which is independent on Ni^{+2} ions concentration. This peak is followed by an exponential decrease in absorption. Evaluation of XRD well-known shows that Ni^{+2} ions substitute Zn^{+2} ions i.e. we are handling substitution solid solution. In the present case, we can count on that Ni ions are acted upon with the aid of an octahedron field.

Nickel (II) can act upon by octahedral, square-planar and tetrahedral symmetries depending upon the composition [33].The presence of a number of absorption bands and their position not handiest depend on upon crystal structure but also rely upon the chemical composition and the particle morphology [34,35].The absorption band edge of undoped ZnO is observed at 375 nm. Within the present study, the optical absorption ofNi-doped ZnO shows asingle absorption peak at 377 nm (3.77 $x10^{-5}$ cm).Commonly, divalent Ni ions in an octahedral symmetry showcase three main bands at about 8300, 14.080, 24.995 cm^{-1}. Those bands are usually assigned due to the spin-allowed triplet-triplet transitions: [36]

$^3A_{2g}(F) \rightarrow {}^3T_{2g}(F)$, $^3A_{2g}(F) \rightarrow {}^3T_{1g}(F)$ and $^3A_{2g}(F) \rightarrow {}^3T_{1g}(P)$

The obtained data reveal that the observed absorption peak is most likely due to

$^3A_{2g}(F) \rightarrow {}^3T_{1g}(P)$

Where this transition is localized at 26525 cm^{-1}

The optical band gap was calculated using Tauc's relation

$$(\alpha h\nu)^{\frac{1}{n}} = A(h\nu - E_g) \quad \textbf{(4)}$$

Where, hv is the photon energy, E_g is the optical band gap of the film, α is the absorption co-efficient, A is a constant, and the exponent n is corresponding to the type of transition. The exponent n is equal to $\frac{1}{2}, 2, \frac{3}{2}$ *and* 3 according to the allowed indirect, direct, forbidden indirect and forbidden direct band gaps, respectively. The energy band gap of undoped and Ni-doped ZnO can be obtained by plotting $(\alpha h\nu)^2$ versus hν and extrapolating the linear portion of absorption edge to find the intercept with energy axis as shown in Figure 5.

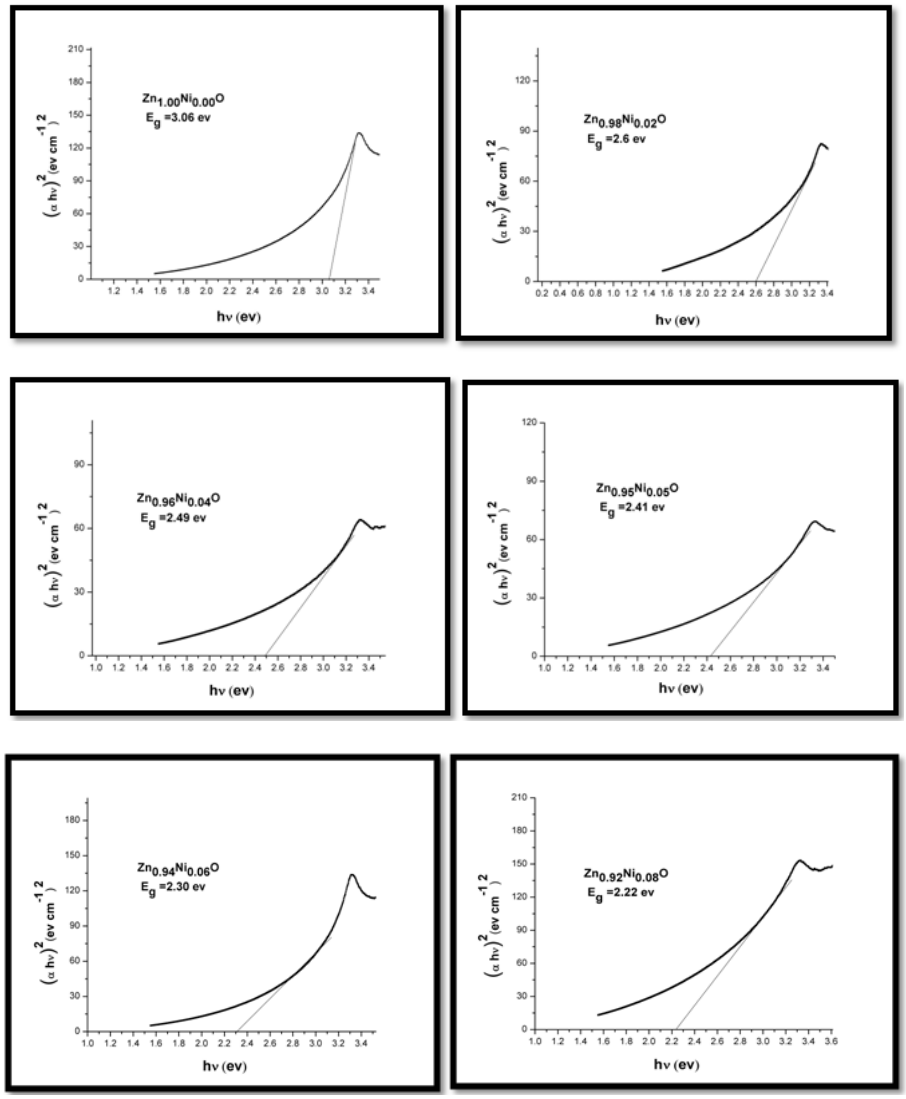

Figure 5: Band Gap Spectra of $Zn_{1-x}Ni_xO$, (x = 0, 0.02, 0.04, 0.05, 0.06 and 0.08)

The observed linear relation between $(\alpha h\nu)^2$in opposition to hν suggests that the direct optical transition is the dominant absorption mechanism. This is an acceptable result, since in crystalline systems the Hamiltonian commute with the operators of symmetry (i.e. the momentum)is conserved and is an integer quantum number. This means that the direct transition is the most probable. Band gap of the samples became determined to decrease from 3.06 eV to 2.57 eV with the increase of Ni concentration. It might be due to the increase in the grainsize [37] in addition to the decreasing of the conduction band prompted by using donor level created by the Ni defects [38].

The envisioned energy band gaps of undoped and Ni-doped ZnO are 3.06 eV, 2.67 eV, 2.49 eV, 2.41 eV, 2.30 eV and 2.22 eV, respectively, as shown in figure 6.

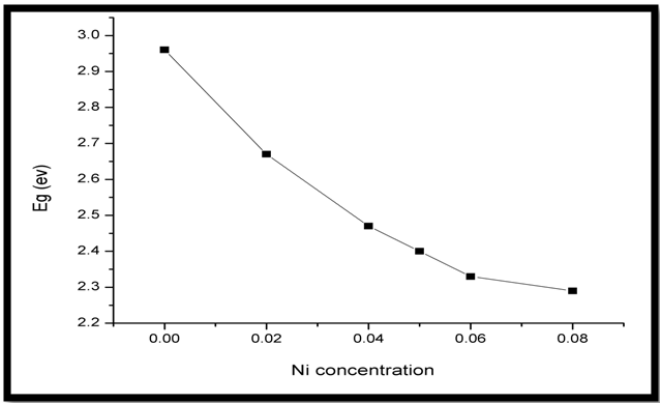

Figure 6: The variation of energy gap of $Zn_{1-x}Ni_xO$, (x = 0, 0.02, 0.04, 0.05, 0.06 and 0.08) as a Function of Ni Concentrations

$Zn_{1-x}Ni_xO$ (where x = 0, 0.02, 0.04, 0.05, 0.06 and 0.08) exhibits red shift with increasing Ni content, i.e. the band gap decreases with increasing the Ni concentration. The decrease in the band gap may be additionally due to the sp-d exchange interactions among the band electrons and the localized d electrons of the substituted divalent ions [39-43].

The truth that Ni^{+2} ions substitute Zn^{+2} ions i.e. we are handling substitutional solid solution. This allows applying rigid band model. Subsequently, the shape of Brillioun zone is fixed and the band gap can be slightly changed with small composition change [44]. Accordingly, Ni ions exist in an octahedral crystal field in the divalent valency state without changing the wurtzite crystal structure of ZnO.

CONCLUSIONS

The undoped and Ni-doped ZnO samples were synthesized by way of the chemical co-precipitation method. XRD exhibits that there is no additional peak corresponding to secondary phases of Ni in ZnO. EDX data confirmed the presence of Ni in prepared samples of $Zn_{1-x}Ni_xO$,(where x= 0, 0.02, 0.04, 0.05, 0.06, 0.08). UV-Vis spectroscopy reveals that Ni ions exist in octahedral crystal field in the divalent valence state without changing the wurtzite crystal structure of ZnO. Thus, Ni^{2+} ions substitute Zn^{2+}ions in the crystal lattice.

REFERENCES

1. T. Meron, G. Markovich, *J.'Ferromagnetism in Colloidal Mn^{2+}-Doped ZnO Nanocrystals', Phys. Chem. B.* 109, 20232 (2005).
2. S. Liang, H. Sheng, Y. Liu, Z. Huo, Y. Lu, H. Shen, *J.'ZnO Schottky ultraviolet photodetectors',Cryst. Growth*, 225, 110 (2001).
3. S.T. Shishiyanu, T.S. Shishiyanu, O.I. Lupan, *Sens.'Pure and Sn-, Ga- and Mn-doped ZnO gas sensors working at different temperatures for formaldehyde, humidity, NH_3, toluene and CO', Actuators B*, 107, 379 (2005).
4. M.H. Huang, S.Mao, H. Feick, H. Yan, Y.Wu, H. Kind, E.Weber, R. Russo P. Yang,' Zinc oxide research',*Science*, 292, 1897 (2001).

5. N. Saito, H. Haneda, T. Sekiguchi, N. Ohashi, I. Sakaguchi, K. Koumoto,' Low-Temperature Fabrication of Light-Emitting Zinc Oxide Micropatterns Using Self-Assembled Monolayers',*Adv. Mater.*, 14, 418 (2002).
6. Roussin Lontio Fomekong,n, Patrice Kenfack Tsobnang, Delphine Magnin, Sophie Hermans, Arnaud Delcorte, John Lambi Ngolui,' Mechanism of $Ni_{1-x}Zn_xO$ Formation by Thermal Treatments on NiO Nanoparticles Dispersed over ZnO', Journal of Solid State Chemistry 230,381–389, (2015).
7. S.J. Pearton,D.P.Noron, K.IP,Y.W.Heo,T.Steiner,' Recent progress in processing and properties of ZnO',Prog.Mater.Sci.50,293–340, (2005).
8. B.D. Aleksandra, X.Y.Chen, Y.H.Leung, etal., J.' Nickel-zinc mixed metal oxide : coprecipitation synthesis and application as gas sen',Mater. Chem.22, 6526–6535,(2012).
9. M. Amir, M.Andrew, C.Micheal, etal. 'Zinc oxide particles: Synthesis, properties and applications', Chem. Eng.J.185, 1–22,(2012).
10. E.R. Beach, K.Shqau, S.E.Brown, S.J.Rozeveld, P.A.Morrisa, 'Nickel-zinc mixed metal oxide: Coprecipitation synthesis and application as gas sensors', Mater. Chem. Phys. 115, 371–377, (2009).
11. D. Adler, J.Feinleib,'Electrical and Optical Properties of Narrow-Band Materials ',Phys.Rev.B2, 3112–3134,(1970).
12. Mergoramadhayenty Mukhtar, LusitraMunisa, Rosari Saleh, Materials Sciences and Applications, 3, 543-551,(2012).
13. R.R. Galazka, Inst. Phys. Conf. Ser. 43, 133 (1979).
14. M. El-Hilo, A.A. Dakhel, A.Y. Ali-Mohamed, J. Magn. Magn.' Room temperature ferromagnetism in nanocrystalline Ni-doped ZnO synthesized by co-precipitation',Mater. 321, 2279 (2009).
15. M. Venkatesan, C.B. Fizgerald, J.G. Lunney, J.M.D. Coey,' Anisotropic Ferromagnetism in Substituted Zinc Oxide', Phys. Rev. Lett. 93, 177206 (2004).
16. X.X. Liu, F.T. Lin, L.L. Sun, W.J. Cheng, X.M. Ma, W.Z. Shi, 'Doping concentration dependence of room-temperature ferromagnetism for Ni-doped ZnO thin films prepared by pulsed-laser deposition',Appl. Phys. Lett. 88, 062508 (2006).
17. D. Karmakar, S.K. Mandal, R.M. Kadam, P.L. Paulose, A.K. Rajarajan, T.K. Nath, A.K. Das, I. Dasgupta, G.P. Das, 'Ferromagnetism in Fe-doped ZnO nanocrystals: experiment and theory', Phys. Rev. B 75, 144,404, (2007).
18. C.W. Cheng, G.Y. Xu, H.Q. Zhang, Y. Luo, 'Hydrothermal synthesis Ni-doped ZnO nanorods with room-temperature ferromagnetism', Material Letters, 62, 1617-1620, (2008).
19. Q.P. Zhong, E. Matijevic, J.Mater. 'Preparation of uniform zinc oxide colloids by controlled double-jet precipitation',Chem., **3**, 443, (1996).
20. W. Lingna, M. Mamoun,' Synthesis of zinc oxide nanoparticles with controlled morphology', J.Mater. Chem., **9,** 2871 (1999).

21. D.W. Bhnemann, C. Kormann, M.R. Hoffmann, 'Preparation and characterization of quantum size zinc oxide: a detailed spectroscopic study', J.Phys. Chem., **91,**3789, (1987).
22. Z. Hui, Y.Deren, M. Xiangyang, J.Yujie, X. Jin,' Synthesis of flower-like ZnO nanostructures by an organic-free hydrothermal process', Nanotechnology., **15,** 622, (2004).
23. J.Zhang, L. D. Sun, J.L. Yin, 'Control of ZnO Morphology via a Simple Solution Route',Chem.Mater., **14,** 4172, (2002).
24. W.J. Li, E.W. Shi, Z.W. Yin, 'Hydrothermal preparation of nanometer ZnO powders',J.Mater.Sci.Lett., **20**, 1381, (2001).
25. R. Gopalakrishnan • S. Muthukumaran, 'Nanostructure, optical and photoluminescence properties of $Zn_{1-x}Ni_xO$ nanoclusters by co-precipitation method',J Mater Sci: Mater Electron,24:1069–1080, (2013).
26. Yan Wang, Xiaoming Liao, Zhongbing Huang, Guangfu Yin, Jianwen Gu b, Yadong Yao, 'Preparation and characterization of Ni-doped ZnO particles via a bio assisted process, Colloids and Surfaces A': Physicochem. Eng. Aspects, 372, 165–171,(2010).
27. G.Vijayaprasath, R.Murugan and G.Ravi, 'Structural, Optical and Magnetic Properties of Ni Doped ZnO Nanostructures Prepared by Co-Precipitation Method', International Journal of Chem Tech Research,6,6, 3385-3387,(2014).
28. Askarinejad, A. Morsali, 'Direct ultrasonic-assisted synthesis of sphere-like nanocrystals of spinel Co3O4 and Mn3O4',Ultrason. Sonochem. 16, 124, (2009).
29. S. Muthukumaran, R. Gopalakrishnan,' Structural, optical and photoluminescence properties of $Zn_{1-x}Ce_xO$ (x = 0, 0.05 and 0.1) nanoparticles by sol–gel method annealed under Ar atmosphere', J. Sol-Gel. Sci. Technol.62, 193, (2012).
30. P.P. Hankare, P.A. Chate, D.J. Sathe, P.A. Chavan, V.M. Bhuse,' Effect of thermal annealing on properties of zinc selenide thin films deposited by chemical bath deposition', J. Mater. Sci.: Mater. Electron. 20, 374, (2009).
31. Sato K, Katayama-Yoshida H. 'Stabilization of ferromagnetic states by electron doping in Fe-, Co- or Ni-doped ZnO'. Jpn J Appl Phys 2001;40:L334–6.
32. Xu C, Yang K, Liu Y, Huang L, Lee H, Cho J, et al. 'Buckling and ferromagnetism of aligned Cr-doped ZnO nanorods',J. Phys Chem C 2008;112:19236–41
33. J. LAKSHMANA RAO, G.L.NARENDRA and S.V.J.LAKSHMAN, 'Optical absorption spectra of cobalt (II) and nickel(II) ions in lead acetate glasses', polyhedron,9,12, 1475-1477, (1990).
34. F.A. Sigoli, M.R. Davolos, M.J. Jafelicci,' Morphological evolution of zinc oxide originating from zinc hydroxide carbonate', J. Alloys Compd. 292,262, (1997).
35. S. Hayashi, N. Nakamori, H. Kanamori, 'Generalized Theory of Average Dielectric Constant and Its Application to Infrared Absorption by ZnO Small Particles',J. Phys. Soc. Jpn. 46, 176,(1979).

36. A.paul and R.W. Douglas, phys. Chem. Glasses,8,233,(1967).

37. M.E. Ghazi, M.Izadifard, F.E.Ghodsi, M.Yuonesi, 'Studying Mn-and Ni-doped ZnO thin films synthesized by the sol–gel method', J.Super- cond. Nov.Magn.25,101–108,(2011).

38. S.K. Patil, S.S.Shinde, K.Y.Rajpure, 'Physical properties of spray deposited Ni-doped zinc oxide thin films', Ceram.Int.39, 3901–3907,(2013).

39. S.B. Ogale, R.J. Choudhary, J.P. Buban, S.E. Lofland, S.R. Shinde, S.N. Kale, et al., 'High temperature ferromagnetism with a giant magnetic moment in transparent Co-doped SnO2-□', Phys. Rev. Lett. 91, 07, 7205-7208, (2003).

40. Y.R. Park, K.J. Kim, 'Sputtering growth and optical properties of [100]-oriented tetragonal SnO2 and its Mn alloy films', J. Appl. Phys. 94, 6401-6404, (2003).

41. M. Bouloudenine, N. Viart, S. Colis, A. Dinia, 'Bulk Zn1-xCoxO magentic semiconductors prepared by hydrothermal technique', Chem. Phys. Lett. 397, 73-76, (2004).

42. S. Colis, H. Bieber, S.B. Colin, G. Schmerber, C. Leuvrey, A. Dinia, 'Magnetic properties of Co-doped ZnO diluted magnetic semiconductors prepared by low-temperature mechanosynthesis', Chem. Phys. Lett. 422, 529-533, (2006).

43. A.Bouaine, N. Brihi, G. Schmerber, C.U. Bouillet, S. Colis, A. Dinia, 'Structural, optical and magnetic properties of Co-doped SnO_2 powders synthesized by the coprecipitation technique', J. Phys. Chem. C 111, 2924-2928, (2007).

44. L.F.Mattheiss, 'Energy band for iron transition series', Phys.rev.134, A979-A973, (1964).